WILEY | Hindawi

*Research Article*

# Random Fuzzy Power Flow Analysis for Power System considering the Uncertainties of Renewable Energy and Load Demands

**J. H. Zheng** (iD), **Wenting Xiao, Zhigang Li** (iD), **and Q. H. Wu**

*School of Electric Power Engineering, South China University of Technology, Guangzhou 510640, China*

Correspondence should be addressed to Zhigang Li; lizg16@scut.edu.cn

Due to the strong uncertainties of renewable energy and load demands, the new type of power systems is facing severe challenges in terms of generation control and load dispatch. Considering the uncertainties of the penetrated renewable energy and diversified load demands, this paper proposes a random fuzzy power flow analysis method (RFPF) to exactly depict the impact on the various flows of power systems. In the RFPF, the random fuzzy models of wind turbine generators, photovoltaic generators, and load demands are established utilizing the stochastic probability functions and fuzzy interval to reveal the uncertainties with high precision. Afterwards, the random fuzzy mean value is developed as an index of accuracy, and the fuzzy number of the output variables is extracted under the 95% confidence level. Furthermore, the proposed RFPF model is executed by applying a three-point estimate method (3PE) to figure out the corresponding power flow of the power system, costing less computation burden compared with the Monte Carlo simulation. Simulation studies conducted on the IEEE-33 system verifies the accuracy of the RFPF and the efficiency of the 3PE.

## 1. Introduction

In the context of the "dual carbon" goal, the traditional power system can no longer meet the carbon emission requirements, so it is an inevitable trend of the power industry to promote the new type of power system, gradually using renewable resources, and replacing traditional energy under the premise of safety and reliability [1, 2]. The new type of power system is a power system with the basic characteristics of clean and low-carbon, safe and controllable, flexible and efficient, intelligent and friendly, and open interaction, with the primary goal of meeting the power demand of economic and social development, and with the main task of maximizing the consumption of new energy [3]. The new type of power system with renewable energy sources can save 10.5% of electricity costs and greatly improve the utilization rate of the available energy, and it is a revolution of the conventional power system [4].

In the construction of the new type of power systems, many technologies have emerged for the reduction of carbon emissions and energy consumption, such as hydrogen storage and carbon capture technology [5], among which it is particularly noteworthy that, the proportion of wind turbine (WT), photovoltaic (PV), and other renewable energy generation has increased significantly [6]. However, due to the strong uncertainty of renewable energy itself, its high proportion to the power grid will change the basic form of the power system, and correspondingly produce a strong uncertainty problem of the multitemporal coupling of the power system [7]. The uncertainty features of renewable energy generation will also cause some problems in the construction of the dispatch region [8] and collaborative optimization of the sustainable energy system [9]. On the other hand, the type of load demands tends to be diversified, which is no longer just a simple power load [10]. It may be coupled with gas or heating/cooling subsystems to form an integrated energy system with multienergy complementarity [11, 12]. In the new type of power system, the load-side components mainly include electric vehicles, electric boilers, and heat pumps. Due to the spatiotemporal randomness and

intermittency of the charging behavior of electric vehicles, it will affect the power quality and bring certain fluctuations and impact the operation of the power system [6].

Therefore, the uncertainties introduced by intermittent renewable generators and variable load demands will affect the economy and the security of the power system [13], and it is inevitable and urgent to consider the uncertainties in the power flow analysis. Moreover, engineering practice shows that, the uncertainties of the power system contains both random and fuzzy one [14]. Random uncertainties from wind speed, solar radiation, and so on, are usually modelled by the probability theory. Fuzzy uncertainties due to subjective reasons which are described in words, are often modelled by the fuzzy set theory. They are independent theoretical systems in the field of basic mathematics [15].

Solving the problem of uncertainties in the power system is a basic and hot issue, and scholars have been engaged in this research for a long time. In dealing with the random uncertainties, the probabilistic power flow (PPF) was first proposed by Borkowska in 1974 [16] and developed by Allan [17]. The authors in reference [18] considered the single random factor of wind speed, and used the Monte Carlo Simulation method (MCS) to calculate the PPF in the power system with a wind farm. The authors in reference [19] employed the Nataf inverse transform to consider the correlation of variables, and proposed an improved multi-linear MCS method based on K-means clustering technology for PPF, and the calculation time was greatly shortened. Reference [20] adopted the cumulant method combined with Cornish–Fisher, which required fewer iterations and less computation time while maintaining satisfactory accuracy. In addition, it is also proved that the Cornish–Fisher series expansion works better than the Gram–Charlier for non-Gaussian for random input variable. The authors in reference [12] presented a gradient descent direction iterative method based on cumulants to analyse the PPF of a heterogeneous integrated energy systems. The authors in reference [21] proved that the point estimate method (PE) with $2m + 1$ scheme has precise results, smaller computational burden, and time, compared to MCS and PE with $2m$ scheme. These studies have fully explored the random model of input variables and algorithm of PPF, which lays a foundation for the subsequent studies of double uncertainties.

On the other hand, to consider fuzzy uncertainties in the power system, fuzzy power flow (FPF) developed by Miranda [22, 23] provides an information modeling tool for inaccurate load predictions, model parameters, and system parameters that are neither deterministic nor random. In FPF, the uncertain parameters of the system are represented by fuzzy numbers, such as trapezoidal and triangular fuzzy numbers, and then the FPF calculation is carried on according to the fuzzy number calculation rule, and finally the output variables are obtained in the form of membership function [24]. Most of the earlier work in this area was for radial distribution systems, but the authors in reference [25]

present a fuzzy distribution power flow for the weakly meshed balanced and unbalanced distribution systems, which can handle the simultaneous presence of several uncertainties of input variables such as network parameters, load model coefficients, load forecast, and bus shunts. The authors in reference [26] proposed an improved forward-backward method for FPF in distribution networks, proving that this method has the property of linear convergence for solving FPF in radial distribution networks. These studies have provided ideas for the modeling and analysis of fuzzy uncertainties, and they have applied fuzzy set theory to the power system, which brings great convenience for the understanding and application of the theory.

In recent years, there have been many problems regarding the double uncertainty of random fuzziness, such as transportation problem [27], image repair [28], and the fractional optimization issue [29]. Researchers also have struggled to tackle the random and fuzzy factors of power flow analysis simultaneously, in order to depict the uncertain characteristics with high precision. The credibility theory is a branch of mathematics completed in the field of basic mathematics, providing a rigorous mathematical basis for the comprehensive evaluation of randomness and fuzziness [15]. Then, Liu established the random fuzzy theory in 2009 that fully supported and synthesized these two uncertainties [30], which lays the foundation of the random fuzzy modeling and algorithm. Based on the random fuzzy simulation technology (RFS), the authors in references [31, 32] adopted the simulation method to deal with random fuzziness. The results obtained by this method can be used as the benchmark for the accuracy of other methods, but the computational efficiency decreases as the number of input variables increases. The authors in reference [33] proposed a cumulant PPF calculation method based on the fuzzy incremental method, considering the parameter fuzziness of wind speed and load. The authors in reference [34] employed the cumulant method and the fuzzy simulation technology to calculate RFPF. Nevertheless, the power flow equation still needs to be linearized, so when the system input variable fluctuates greatly, the algorithm error may be larger. The authors in reference [35] established a random fuzzy output model of WT, PV, and load, and proposed a two-stage calculation method based on PE for RFPF, but this method did not extract the fuzzy characteristics of state variables.

Based on these existing works, this study adopts 3PE with RFS to calculate RFPF, considering the random fuzzy two-fold uncertainty of renewable energy and load demands. Based on the random fuzzy theory, this study establishes the random fuzzy model of WT, PV, and load demands, and extracts the triangular fuzzy numbers of the output variables, so as to obtain their membership functions. At the same time, the probabilistic density function (PDF) and cumulative distribution function (CDF) of the state variables are obtained by the Cornish–Fisher series expansion theory. Moreover, the proposed RFPF model is executed by applying

a 3PE to describe the corresponding power flow of the power system, costing less computation burden compared with the Monte Carlo simulation. Finally, the effectiveness of the proposed method is verified in the modified IEEE-33 system.

## 2. Random Fuzzy Model for Power Flow

In order to make the system equation have both randomness and fuzziness, based on the random fuzzy theory, the authors express the input variables of the system equation (such as the output of WT, PV, and load demands) with the random fuzzy models. The detailed modeling process is described below in the study.

### 2.1. Power Flow Formulation Embedded with WT and PV.
In this study, the AC power flow formulation is utilized to calculate the random fuzzy power flow. Hence, the active and reactive power injection at each bus can be written as

$$\text{Real}\left(V\left(YV\right)^{*}\right) - P_{S} = 0, \tag{1}$$

$$P_{S} = P_{\text{gen}} + P_{\text{WT}} + P_{\text{PV}} - P_{\text{LD}}, \tag{2}$$

$$\text{Imag}\left(V\left(YV\right)^{*}\right) - Q_{S} = 0, \tag{3}$$

$$Q_{S} = Q_{\text{gen}} - Q_{\text{LD}}, \tag{4}$$

where $V$ is the voltage vector, $Y$ is the node admittance matrix, $P_{\text{gen}}$ and $Q_{\text{gen}}$ denote the active and reactive power of traditional generators, such as hydroelectric generators and thermal generators, $P_{\text{WT}}$ and $P_{\text{PV}}$ are the output of wind turbine generators and photovoltaics, and $P_{\text{LD}}$ and $Q_{\text{LD}}$ represent the electrical load. It is worth noting that, $P_{\text{WT}}$, $P_{\text{PV}}$, $P_{\text{LD}}$, and $Q_{\text{LD}}$ are all random fuzzy variables.

### 2.2. Random Fuzzy Model of Renewable Energy Generators and Load Demands.
Let $\Theta$ be a nonempty set and $P(\Theta)$ the power set of $\Theta$. Each element in $P(\Theta)$ is called an event. $Pos$ denotes the possibility measure. They make up the possible space $(\Theta, P(\Theta), Pos)$. Random fuzzy variable is defined as a function from the possible space $(\Theta, P(\Theta), Pos)$ to random variables [30]. Based on this definition, we can establish random fuzzy model of WT, PV, and load demands.

### 2.2.1. Wind Turbine Generators Model.
We use the Weibull distribution to describe the random feature of wind speed [36] and use the triangular fuzzy number to describe the fuzzy uncertainty of the Weibull parameters [31]. There are the following three reasons:

(i) The two-parameter Weibull PDF has 87.19% to describe the wind speed, which is not fully fit to the historical data [37]

(ii) Because the measuring process of equipments is often affected by some factors such as weather

condition and temperature, most of the historical data would be imprecise

(iii) The deviation between the forecast Weibull PDF and the real one is often described qualitatively and in linguistic, according to the experience of the operator

Thus, the fitting degree of the Weibull distribution and the accuracy of the historical data are not negligible and can be depicted by the fuzzy language mathematically. So, the simplified expression of wind speed can be described as

$$\begin{cases} v(\theta) \sim W(c(\theta), k(\theta)) \\ c, k \sim (r_1, r_2, r_3) \end{cases}, \tag{5}$$

where $W$ represents the Weibull PDF, $v$ denotes wind speed which is random fuzzy variables, $\theta$ is the element from possible space, and $k$ and $c$ are both triangular fuzzy numbers.

Moreover, triangular fuzzy number is fully determined by the triplet $(r_1, r_2, r_3)$ of crisp numbers with $r_1 < r_2 < r_3$ [30], whose membership function is given by

$$\mu(\theta) = \begin{cases} \dfrac{\theta - r_1}{r_2 - r_1}, & \text{if } r_1 \leq \theta \leq r_2 \\[2mm] \dfrac{\theta - r_3}{r_2 - r_3}, & \text{if } r_2 \leq \theta \leq r_3. \\[2mm] 0, & \text{otherwise.} \end{cases} \tag{6}$$

Then, we can achieve the detailed formulation of the random fuzzy model of the wind speed [35]

$$f(v) = \frac{\xi_k}{\xi_c} \left(\frac{v}{\xi_c}\right)^{\xi_k - 1} \exp\left[-\left(\frac{v}{\xi_c}\right)^{\xi_k}\right], \tag{7}$$

$$\xi_k, \xi_c \sim (r_1, r_2, r_3),$$

where $\xi_k$ and $\xi_c$ are, respectively, the shape and scale parameters, and they are triangular fuzzy variables.

The functional relationship between the output of WT generators and wind speed can be evaluated by

$$P_{\text{WT}} = \begin{cases} 0 & v \leq v_{\text{in}} \text{ or } v \leq v_{\text{out}} \\ k_1 v + k_2 & v_{\text{in}} \leq v \leq v_{\text{r}} \\ P_{\text{rw}} & v_{\text{r}} \leq v < v_{\text{out}} \end{cases}, \tag{8}$$

where $P_{\text{WT}}$ is the actual output of WT, $P_{\text{rw}}$ is the rated power of WT, $v_{\text{in}}$, $v_{\text{r}}$, and $v_{\text{out}}$ are the cut-in, rated, and cut-out wind speed, respectively. $k_1$ and $k_2$ are evaluated as

$$k_1 = \frac{P_{\text{rw}}}{v_{\text{r}} - v_{\text{in}}}, k_2 = -k_1 v_{\text{in}}. \tag{9}$$

Based on the statistics, the wind speed usually falls into the range $v_{\text{in}}$ to $v_{\text{r}}$, so the $P_{\text{WT}}$ is approximation a linear

function of $v$ [38]. The random fuzzy model of the output of WT in equation (2) is formulated by

$$f(P_{\text{WT}}) = \frac{\xi_{\text{k}}}{k_1}\left(\frac{P_{\text{WT}} - k_2}{k_1\xi_{\text{c}}}\right)^{\xi_{\text{k}} - 1} \exp\left[-\left(\frac{P_{\text{WT}} - k_2}{k_1\xi_{\text{c}}}\right)^{\xi_{\text{k}}}\right]. \tag{10}$$

*2.2.2. Photovoltaic Generators Model.* Similar to the above process, we can build the random fuzzy model of the output of PV generators. The best distribution function to depict the regular of the solar radiance is the Beta PDF. The solar radiance random fuzzy model [34] can be modeled as

$$T(r) = \frac{\Gamma(\xi_{\text{a}} + \xi_{\text{b}})}{\Gamma(\xi_{\text{a}})\Gamma(\xi_{\text{b}})}\left(\frac{r}{r_{\max}}\right)^{\xi_{\text{a}} - 1}\left(1 - \frac{r}{r_{\max}}\right)^{\xi_{\text{b}} - 1}, \tag{11}$$

$$\xi_{\text{a}}, \xi_{\text{b}} \sim (r_1, r_2, r_3),$$

where $\Gamma$ is the Gamma function; $r$ and $r_{\max}$ are, respectively, the actual and maximum solar radiance; $\xi_{\text{a}}$ and $\xi_{\text{b}}$ are the shape parameters of Beta PDF which are both triangular fuzzy variables.

Then, the random fuzzy model of output of PV is formulated by

$$T(P_{\text{PV}}) = \frac{\Gamma(\xi_{\text{a}} + \xi_{\text{b}})}{\Gamma(\xi_{\text{a}})\Gamma(\xi_{\text{b}})}\left(\frac{P_{\text{PV}}}{R_{\text{M}}}\right)^{\xi_{\text{a}} - 1}\left(1 - \frac{P_{\text{PV}}}{R_{\text{M}}}\right)^{\xi_{\text{b}} - 1}, \tag{12}$$

where $P_{\text{PV}}$ is the actual solar generation output and $R_{\text{M}}$ is the maximum power available from the modules. The power factor of PV is approximately 1.

*2.2.3. Load Demands Model.* The load demands are often modeled as a normal distribution function [39], and their random fuzzy model can be formulated by

$$f(P_{\text{L}}) = \frac{1}{\sqrt{2\pi}\xi_{\sigma\text{P}}}\exp\left(-\frac{(P_{\text{L}} - \xi_{\mu\text{P}})^2}{2\xi_{\sigma\text{P}}^2}\right),$$

$$f(Q_{\text{L}}) = \frac{1}{\sqrt{2\pi}\xi_{\sigma\text{Q}}}\exp\left(-\frac{(Q_{\text{L}} - \xi_{\mu\text{Q}})^2}{2\xi_{\sigma\text{Q}}^2}\right), \tag{13}$$

$$\xi_{\mu\text{P}}, \xi_{\sigma\text{P}}, \xi_{\mu\text{Q}}, \xi_{\sigma\text{Q}} \sim (r_1, r_2, r_3),$$

where $P_{\text{L}}$ and $Q_{\text{L}}$ are the active and reactive load powers, respectively, $\xi_{\mu\text{P}}$ and $\xi_{\mu\text{Q}}$ are the mean of the active power and the reactive power, respectively, and $\xi_{\sigma\text{P}}$ and $\xi_{\sigma\text{Q}}$ are the standard deviations of the active power and the reactive power, respectively, which are triangular fuzzy variables.

## 3. Calculation of Random Fuzzy Power Flow Using 3PE

*3.1. The Brief Principle of 3PE.* The PE selects some estimated points that can reflect the digital characteristics of the input variable through the numerical method, so that the output points can also approximate the digital characteristics of the output variable. This can greatly reduce the number of samples and improve the calculation efficiency.

When the selected estimated point $m$ is 2, the accuracy of the algorithm is low; when $m \geq 4$, the number of samples is too large, resulting in low-computational efficiency, and high-order moments are difficult to solve. However, when $m = 3$, the algorithm can obtain more accurate results in a short time. Therefore, 3PE is taken in this study for power flow calculation [40].

In the 3PE, calculating the estimated points and their weights is the most important step.

Suppose that the input random variables $(x_1, x_2, \ldots, x_n)$ are independent of each other, and then we can get three estimated points based on the following equation:

$$x_{k,i} = \mu_k + l_{k,i}\delta_k, i = 1, 2, 3; k = 1, 2, \ldots, n, \tag{14}$$

where $\mu_k$ and $\delta_k$ are the mean and standard deviation of the input random variable $x_k$. The location $l_{k,i}$ is determined by

$$\begin{cases} l_{k,i} = \frac{\lambda_{k,3}}{2} + (-1)^{3-i}\sqrt{\lambda_{k,4} - \frac{3\lambda_{k,3}^2}{4}}, i = 1, 2, \\ \\ l_{k,3} = 0, \end{cases} \tag{15}$$

where $\lambda_{k,3}$ and $\lambda_{k,4}$ denote the 3rd and 4th standard central moment of the random variable $x_k$ with PDF $f_k$, that is calculated by equation (16). They are also called the skewness and kurtosis of the input random variable $x_k$

$$\begin{cases} \lambda_{k,3} = \frac{\int_{-\infty}^{\infty}(x_k - \mu_k)^3 f_k dx_k}{(\delta_k)^3} \\ \\ \lambda_{k,4} = \frac{\int_{-\infty}^{\infty}(x_k - \mu_k)^4 f_k dx_k}{(\delta_k)^4} \end{cases}. \tag{16}$$

Then, the weight $w_{k,i}$ can be figured out by

$$\begin{cases} w_{k,i} = \frac{(-1)^{3-i}}{\left(l_{k,i}(l_{k,1} - l_{k,2})\right)}, i = 1, 2 \\ \\ w_{k,3} = \frac{1}{n} - w_{k,1} - w_{k,2} = \frac{1}{n} - \frac{1}{\lambda_{k,4} - \lambda_{k,3}^2} \end{cases}. \tag{17}$$

Once the estimation points $x_{k,i}$ and weights $w_{k,i}$ of input random variable $x_k$ are obtained, the functions (1–4) are evaluated at points $(\mu_1, \mu_2, \ldots, x_{k,i}, \ldots, \mu_n)$ by the Newton–Raphson method yielding $Z(k, i)$, where $Z$ is the vector of output random variables.

Finally, by using the weighting factors $w_{k,i}$ and $Z(k, i)$ values, the $j$th raw moment of the output random variables can be estimated according to the expression:

$$E_{pro}(Z^j) = \sum_{k=1}^{n} \sum_{i=1}^{3} w_{k,i} \times \left[ f(\mu_1, \mu_2, \ldots, x_{k,i}, \ldots, \mu_n)^j \right].$$
(18)

*3.2. Random Fuzzy Simulation.* Suppose $\xi$ is a random fuzzy variable in the possible space $(\Theta, P(\Theta), Pos)$ and $f$ is a measurable function, then, $\forall \theta \in \Theta$, the random fuzzy mean value of $\xi$ is defined as

$$E_{\text{pro–fuz}}[\xi] = \int_0^{\infty} \text{Cr}\{E_{\text{pro}}(f(\xi(\theta))) \geq r\} dr$$
$$- \int_{-\infty}^{0} \text{Cr}\{E_{\text{pro}}(f(\xi(\theta))) \leq r\} dr,$$
(19)

where $\text{Cr}\{\cdot\}$ denotes the credibility measure.

RFS can be used to obtain random fuzzy mean value $E_{\text{pro–fuz}}$ as shown in Algorithm 1[41], where $\vee$ is the maximum operator, $\wedge$ is the minimum operator, and O denotes null set.

*3.3. The Process of 3PE-RFS*

*3.3.1. The Flowchart of 3PE-RFS.* In order to deal with the two uncertainties, this study combines the three-point estimate method and random fuzzy simulation technology (3PE-RFS) to calculate the RFPF.

Suppose $N$ is the number of samples of the fuzzy number. $W$, $B$, and $N$ are represented Weibull, beta, and normal distribution separately. The flowchart of 3PE-RFS and the processing of output results are shown in Figure 1.

*3.3.2. Detailed Algorithm Process.* The algorithm process is briefly described as sampling, power flow calculation, and processing output stage.

The sampling stage is shown in the red shade in Figure 1, and the specific process is as follows:

(1) According to triangular fuzzy number $(r_1, r_2, r_3)$, we can write the corresponding membership function like formula (6). Then, a series of fuzzy samples of $(\xi_c, \xi_k)$, $(\xi_a, \xi_b)$, and $(\xi_\mu, \xi_\sigma)$ are randomly drawn from the possibility space, each corresponding to a membership degree [31, 34, 41].

(2) With one set of fuzzy sample of parameters, we can obtain PDF of output of WT, PV, and load described in (10)–(13)

(3) Based on the distribution obtained, three estimated points of 3PE will be figured out in the probability space according to (14)–(17)

The power flow calculation stage is shown in the yellow shade in Figure 1, and the specific process is as follows:

(1) Under each set of fuzzy parameters, the 3PE probability power flow calculation is carried out with these three estimated points based on the Newton–Raphson method to solve the nonline equations (1)–(4). The iteration function is as follows:

$$\begin{cases} \Delta F = J * \Delta X \\ X^{(i+1)} = X^{(i)} - \Delta X^{(i)} \end{cases},$$
(20)

where $\Delta F$ is the mismatch calculated by (21), $X$ is the state variables including voltage amplitude and voltage angle, $J$ denotes Jacobian matrix, and $i$ represents the number of iterations.

$$\Delta F = \begin{cases} \Delta P = \text{Real}(V(YV)^*) - P_S = 0 \\ \Delta Q = \text{Imag}(V(YV)^*) - Q_S = 0. \end{cases}$$
(21)

(2) A random mean value $E_{\text{pro},i}(Z)$ of the state variable $Z$ based on (18) is obtained

(3) This calculation process will be performed $N$ times and obtain $N$ values of $E_{\text{pro},i}(Z)$

The output procedure stage is as follows:

(1) Calculating the random fuzzy mean value $E_{\text{pro–fuz}}(Z)$ with $E_{\text{pro},i}(Z)$ as mentioned in the section "Random fuzzy simulation," and the process is shown in the green shade in Figure 1

(2) On the other hand, in order to extract the triangular fuzzy numbers $(r_1, r_2, r_3)$ of mean value of output variables which can derive their membership functions, the confidence interval of $E_{\text{pro},i}(Z)$ under the 95% confidence level is obtained, and find the approximate center of the interval as $r_2$ is found, and the minimum lower limit is set as $r_1$ and the maximum upper limit is set as $r_3$ [32], which is shown in the blue shade in Figure 1.

# 4. Case Study

*4.1. Parameter Setting and Performance Test.* The method proposed in this study is simulated in the modified IEEE-33 system [35], compared with MCS based on the random fuzzy simulation technology (MCS-RFS). There are 2 wind turbine generators located at bus 13 and bus 23, and one photovoltaic generator installed at bus 28, respectively. The rated power of WT and PV is 0.2 MW.

For wind turbine generators, the $V_{\text{in}}$, $V_r$, and $V_{\text{out}}$ are 4 m/s, 15 m/s, and 25 m/s, respectively. The number of fuzzy sample is 100. The range of the fuzzy parameters is set to $(99\%r_2, r_2, 101\%r_2)$, which uses (99%, 101%) for short and $r_2$ is the mean value of the fuzzy parameter.

```
(1)  e = 0;
(2)  θ = rand([1 n]), satisfying (θ) ≤ ϵ (ϵ > 0);
(3)  Calculate E_pro(f(ξ(θ)));
(4)  a = min_{1≤i≤n} E_pro(f(ξ(θ)));
(5)  b = max_{1≤i≤n} E_pro(f(ξ(θ)));
(6)  r = a + (b − a) ∗ rand([1 n]) ∈ (a, b);
(7)  for i = 1: n do
(8)     if r(i) ≥ 0 then
(9)        e = e + Cr{θ ∈ Θ | E_pro(f(ξ(θ))) ≥ r};
(10)    else
(11)       e = e − Cr{θ ∈ Θ | E_pro(f(ξ(θ))) ≤ r};
(12)  E_{pro−fuz}(f(ξ(θ))) = a∨O + b∧O + e × (b − a)/n
```

ALGORITHM 1: The algorithm of RFS.
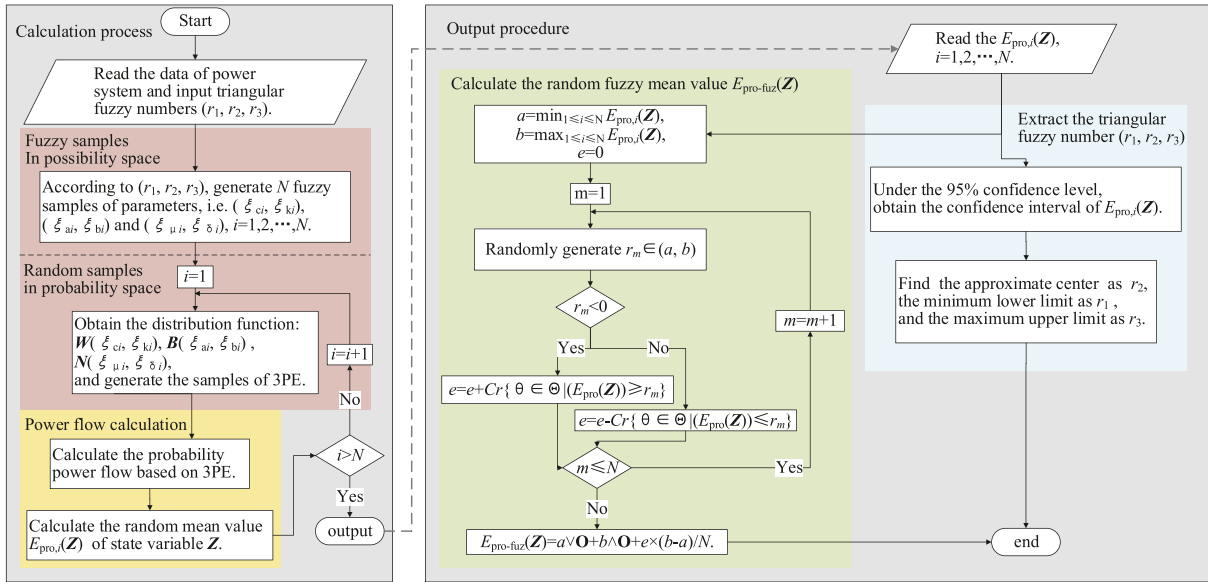


FIGURE 1: Flowchart of the calculation process of 3PE-RFS.

In order to simplify the description, the simulation process takes only the random fuzziness of load as an example.

According to the interval (99%, 101%), 100 fuzzy samples of parameter $(\xi_\mu, \xi_\sigma)$ are selected in the possibility space as shown in Figures 2(a) and 2(b), and they are subject to triangular membership function.

Under each set of fuzzy samples, the random samples of load are obtained, which follow the normal distribution, as shown in Figure 2(c). The number of random samples is 300 of MCS-RFS, while that of the proposed method is 71. These samples are used to calculate the PPF and obtain the random mean value $E_{\text{pro},i}(Z)$ and the variance value $\text{Var}_{\text{pro},i}(Z)$ of the state variable $Z$. This calculation process is done 100 times.

Finally, $E_{\text{pro},i}(Z)$ and $\text{Var}_{\text{pro},i}(Z)$ are used for the following processing:

(i) On the one hand, the random fuzzy mean $E_{\text{pro−fuz}}(Z)$ is calculated, which is used to compare with MCS-RFS

(ii) On the other hand, obtaining their triangular fuzzy number, which is used to compare with 3PE

### 4.1.1. Comparison between 3PE-RFS and MCS-RFS.
In order to verify the accuracy of the proposed method, the relative error of $E_{\text{pro−fuz}}(Z)$ is used as an indicator for the comparison of the two methods [42], as shown in the given equation, and the results are drawn in Figure 3.

$$X_* = \left| \frac{X_{\text{3PE−RFS}} − X_{\text{MCS−RFS}}}{X_{\text{MCS−RFS}}} \right| \times 100\%, \qquad (22)$$

where $X_*$ denotes the relative errors of $E_{\text{pro−fuz}}(Z)$, $X_{\text{3PE−RFS}}$, and $X_{\text{MCS−RFS}}$ are $E_{\text{pro−fuz}}(Z)$ of the proposed method and MCS-RFS. $X$ represents the state variable, such as voltage amplitude $V_{\text{m}}$, voltage angle $V_{\text{a}}$, active power of lines $P_{\text{line}}$, and reactive power of lines $Q_{\text{line}}$.

It can be seen intuitively from Figure 3 that the maximum value of $X_*$ of $V_{\text{m}}$, $V_{\text{a}}$, $P_{\text{line}}$, and $Q_{\text{line}}$ do not exceed 0.005%, 0.14%, 0.1%, and 0.09%, respectively, which shows
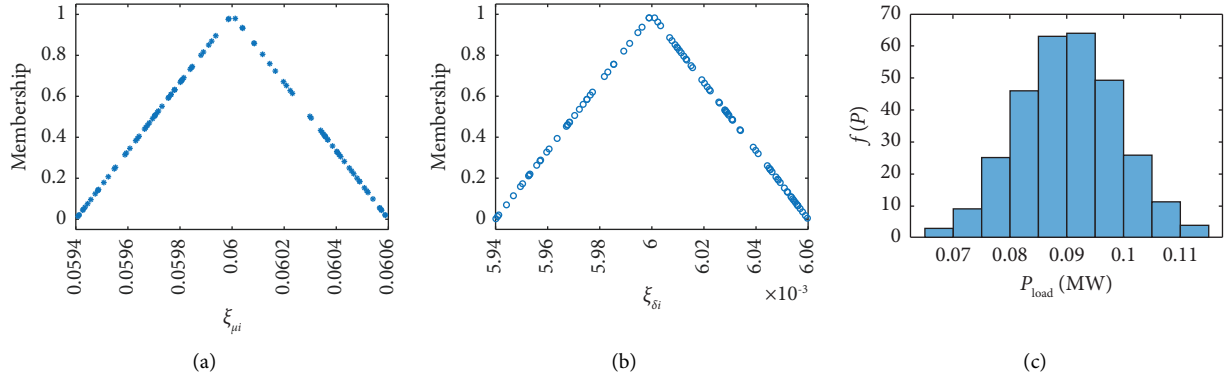
FIGURE 2: Fuzzy and random sample of loads. (a) Parameter $\mu$. (b) Parameter $\sigma$. (c) Active power of loads.
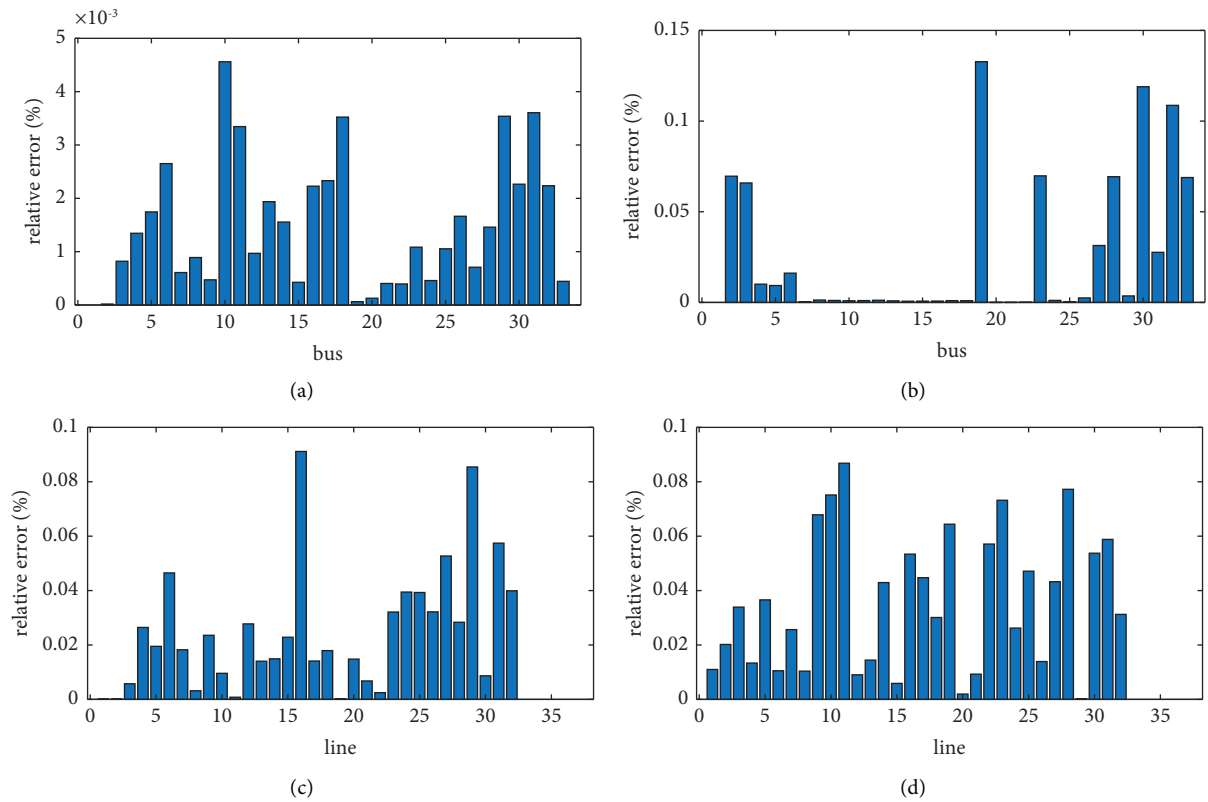


FIGURE 3: Relative errors of random fuzzy mean of two methods. (a) $V_m$. (b) $V_a$. (c) $P_{line}$. (d) $Q_{line}$.

that the proposed method has extremely high accuracy. On the other hand, the time consumed by MCS-RFS is 230 s, while the proposed method just needs 63 s, which shows that the proposed method has relatively faster calculation speed.

### 4.1.2. Comparison between 3PE-RFS and 3PE.

In order to compare the difference in output between 3PE-RFS and 3PE, we record the mean and variance values of $V_m$ of the two

methods in Table 1 and unify the variance value into units of $(1e - 3)$ for easy observation.

Since bus 1 is selected as the slack bus, $V_m$ of bus 1 is a specified value and its mean or variance is 0. The results at other buses in Table 1 presents that the mean and variance of $V_m$ are a fixed value in 3PE, but that of 3PE-RFS is triangular fuzzy numbers.

In order to more clearly display the relationship between the two method, we draw the picture of the membership

TABLE 1: Mean and variance of $V_m$.

| Bus | 3PE | | 3PE-RFS | |
| --- | --- | --- | --- | --- |
| | Mean | Variance ($1e-3$) | Mean | Variance ($1e-3$) |
| 1 | 0.00000 | 0.0000 | (0, 0, 0) | (0, 0, 0) |
| 2 | 0.99703 | 0.0730 | (0.99702, 0.99703, 0.99704) | (0.0727, 0.0729, 0.0732) |
| 3 | 0.98294 | 0.4532 | (0.98288, 0.98293, 0.98301) | (0.4514, 0.4525, 0.455) |
| 4 | 0.97545 | 0.6336 | (0.97537, 0.97544, 0.97556) | (0.6317, 0.6336, 0.6367) |
| 5 | 0.96806 | 0.8328 | (0.96794, 0.96803, 0.96819) | (0.8303, 0.8322, 0.8374) |
| 6 | 0.94965 | 1.3969 | (0.94946, 0.94959, 0.94988) | (1.3923, 1.3966, 1.4065) |
| 7 | 0.94617 | 1.4700 | (0.94596, 0.94611, 0.94641) | (1.4656, 1.47, 1.4795) |
| 8 | 0.94132 | 1.5679 | (0.9411, 0.94126, 0.94158) | (1.5638, 1.5688, 1.5775) |
| 9 | 0.93505 | 1.6837 | (0.93481, 0.93504, 0.93534) | (1.6807, 1.6858, 1.6941) |
| 10 | 0.92924 | 1.8127 | (0.92898, 0.92923, 0.92954) | (1.8108, 1.816, 1.8243) |
| 11 | 0.92838 | 1.8336 | (0.92811, 0.92835, 0.92868) | (1.8318, 1.837, 1.8454) |
| 12 | 0.92688 | 1.8723 | (0.92661, 0.92685, 0.92719) | (1.8707, 1.8762, 1.8844) |
| 13 | 0.92076 | 2.0520 | (0.92047, 0.92073, 0.92111) | (2.0513, 2.0569, 2.0664) |
| 14 | 0.91850 | 2.1286 | (0.91819, 0.91847, 0.91885) | (2.1283, 2.1334, 2.1442) |
| 15 | 0.91708 | 2.1664 | (0.91677, 0.91705, 0.91744) | (2.1664, 2.1723, 2.1825) |
| 16 | 0.91572 | 2.2072 | (0.9154, 0.91569, 0.91608) | (2.2077, 2.2139, 2.2241) |
| 17 | 0.91369 | 2.2784 | (0.91336, 0.91366, 0.91406) | (2.2795, 2.2853, 2.2969) |
| 18 | 0.91308 | 2.3050 | (0.91275, 0.91303, 0.91346) | (2.3065, 2.3122, 2.3244) |
| 19 | 0.99650 | 0.0820 | (0.99649, 0.9965, 0.99652) | (0.0818, 0.082, 0.0823) |
| 20 | 0.99293 | 0.2531 | (0.99289, 0.99292, 0.99296) | (0.253, 0.2539, 0.2559) |
| 21 | 0.99222 | 0.2939 | (0.99218, 0.99221, 0.99227) | (0.2932, 0.2942, 0.2968) |
| 22 | 0.99158 | 0.3361 | (0.99154, 0.99157, 0.99164) | (0.3346, 0.3361, 0.3392) |
| 23 | 0.97935 | 0.6307 | (0.97926, 0.97933, 0.97945) | (0.6267, 0.6283, 0.6334) |
| 24 | 0.97268 | 1.0616 | (0.97253, 0.97265, 0.97284) | (1.0522, 1.0565, 1.067) |
| 25 | 0.96935 | 1.3116 | (0.96917, 0.96931, 0.96955) | (1.2982, 1.3034, 1.3188) |
| 26 | 0.94772 | 1.4749 | (0.94752, 0.94766, 0.94796) | (1.4698, 1.4745, 1.4854) |
| 27 | 0.94516 | 1.5855 | (0.94494, 0.94509, 0.94542) | (1.5797, 1.5842, 1.5972) |
| 28 | 0.93372 | 2.1603 | (0.93342, 0.93366, 0.93406) | (2.1507, 2.1578, 2.1791) |
| 29 | 0.92550 | 2.6092 | (0.92514, 0.92538, 0.92591) | (2.5968, 2.6049, 2.6333) |
| 30 | 0.92194 | 2.8122 | (0.92155, 0.92183, 0.92239) | (2.7983, 2.8124, 2.8385) |
| 31 | 0.91778 | 2.9545 | (0.91737, 0.91766, 0.91825) | (2.9401, 2.9549, 2.9795) |
| 32 | 0.91686 | 2.9901 | (0.91646, 0.91674, 0.91734) | (2.9754, 2.9885, 3.0147) |
| 33 | 0.91658 | 2.9951 | (0.91617, 0.91646, 0.91705) | (2.9804, 2.9953, 3.0197) |
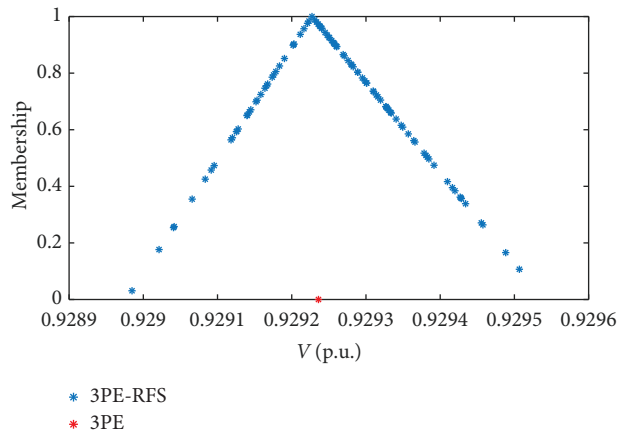


(a)
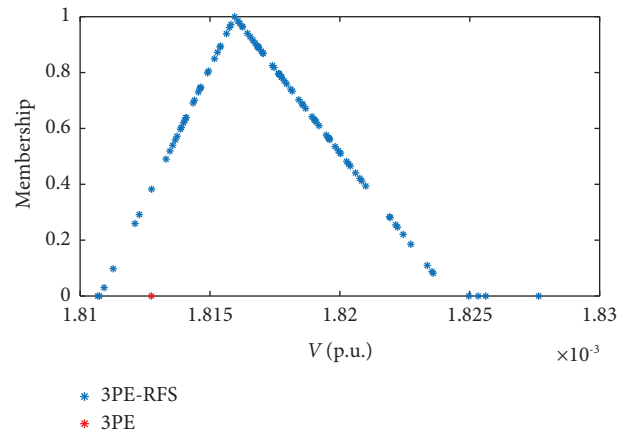


(b)

FIGURE 4: Membership function of $V_m$ of bus 10. (a) Mean value. (b) Variance value.

function of the mean and variance of $V_m$, as shown in Figure 4, which shows that the result of 3PE is just a single point in the result interval of 3PE-RFS.

Although a very small amount of the data of 3PE is not included in this interval, such as the situation of bus 16, most of the data are included in the results of 3PE-RFS. This is
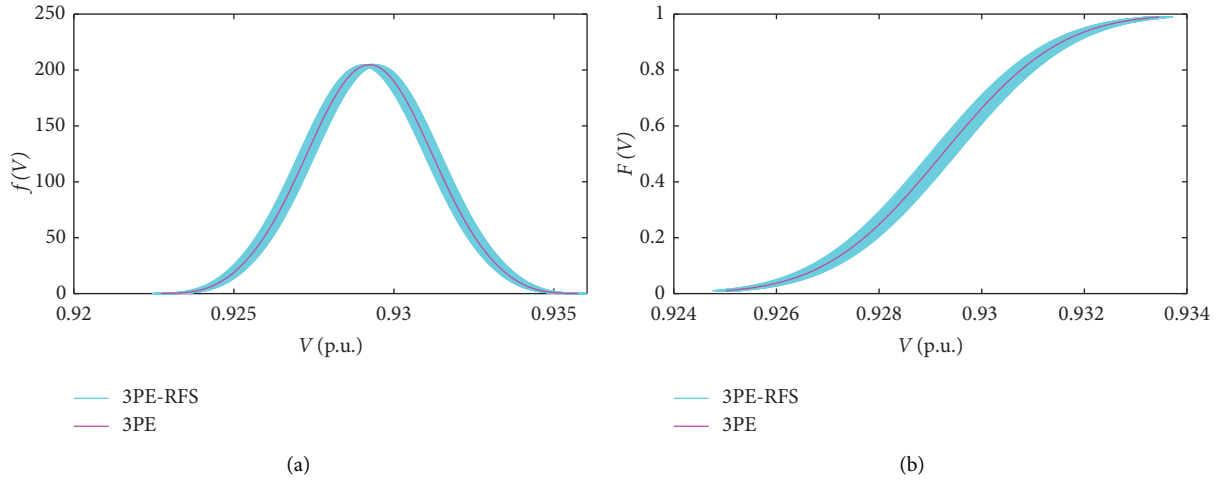
FIGURE 5: The PDF and CDF images of $V_m$ of bus 10. (a) PDF. (b) CDF.
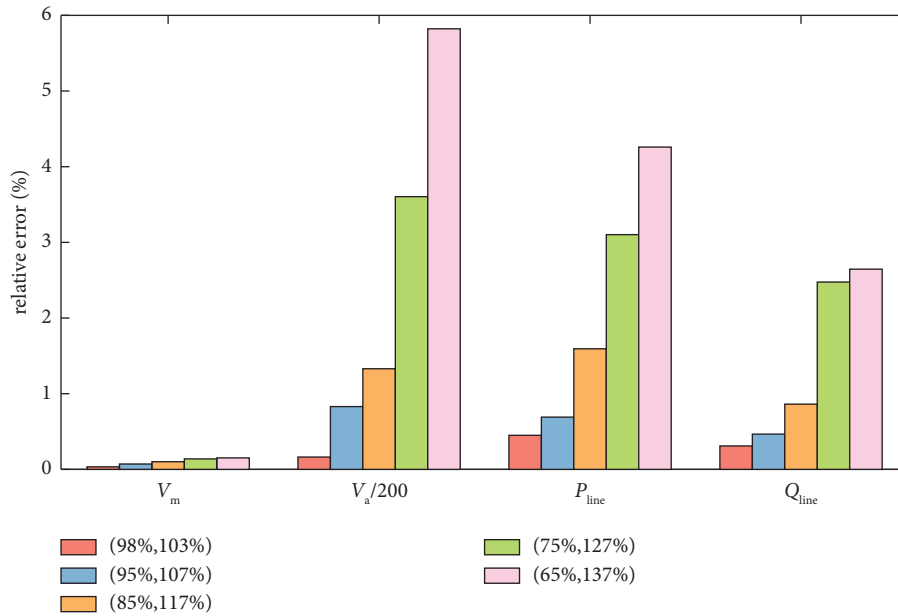


FIGURE 6: The mean value of $X_*$ with different ranges of fuzzy parameter.

because the result of 3PE-RFS in Table 1 is a set of triangular fuzzy numbers obtained at the 95% confidence interval.

Taking the help of the Cornish–Fisher series expansion theory, we draw the PDF and CDF images of bus 10 in Figure 5, and it shows that the PDF and CDF images of 3PE-RFS are no longer a single curve such as 3PE but in the form of cluster.

As can be seen from the aforementioned comparison, the results obtained by 3PE-RFS include that of 3PE, which means when the actual value of the load output deviates from the predicted value or the output of WT and PV fluctuates sharply, the results of 3PE are likely to deviate from the actual value, if a single PDF curve is used to analyze the operating characteristics of the system by only considering the randomness.

When the random fuzziness is considered, the decision set of PDF curves can be obtained, and the operators can make decisions on fuzzy parameters according to the actual operation of the system and different risk preferences, and the decision plan is more reasonable than a single curve.

*4.1.3. The Impact of Fuzzy Factor.* In order to analyse the effect of increasing volatility on the system, the range of fuzzy parameters of WT, PV and load is set to (99%, 101%), (98%, 103%), (95%, 107%), (85%, 117%), (75%, 127%), and (65%, 137%).

Taking the result of (99%, 101%) as a reference, the authors calculate the mean value of $X_*$ of each state variable, as shown in Figure 6.
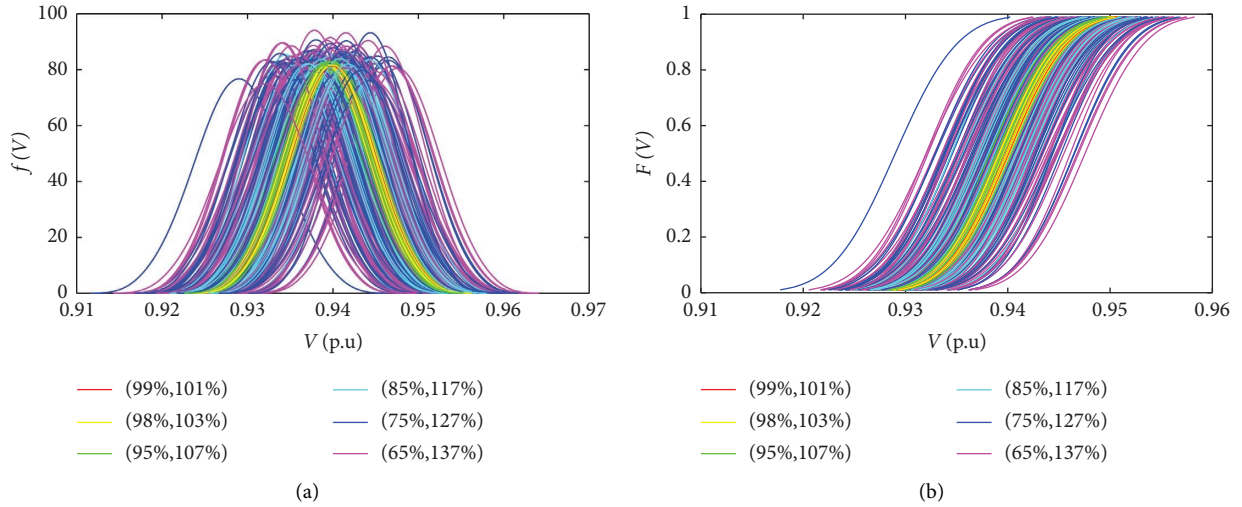
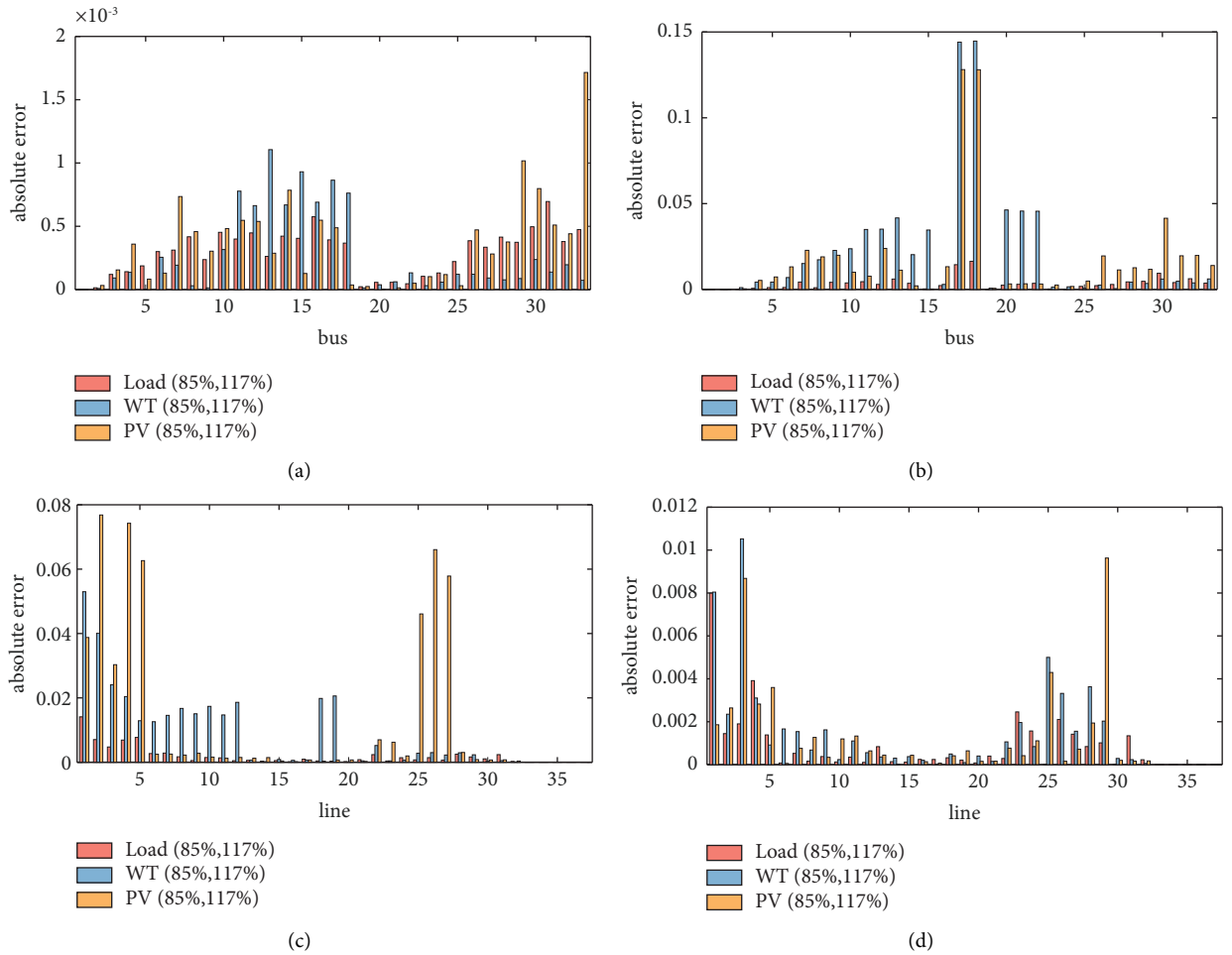FIGURE 7: The PDF and CDF images of $V_m$ of bus 10 with different ranges of fuzzy parameter. (a) PDF. (b) CDF.



FIGURE 8: The absolute errors of state variables with different kinds of fuzzy factor increase. (a) $V_m$. (b) $V_a$. (c) $P_{line}$. (d) $Q_{line}$.
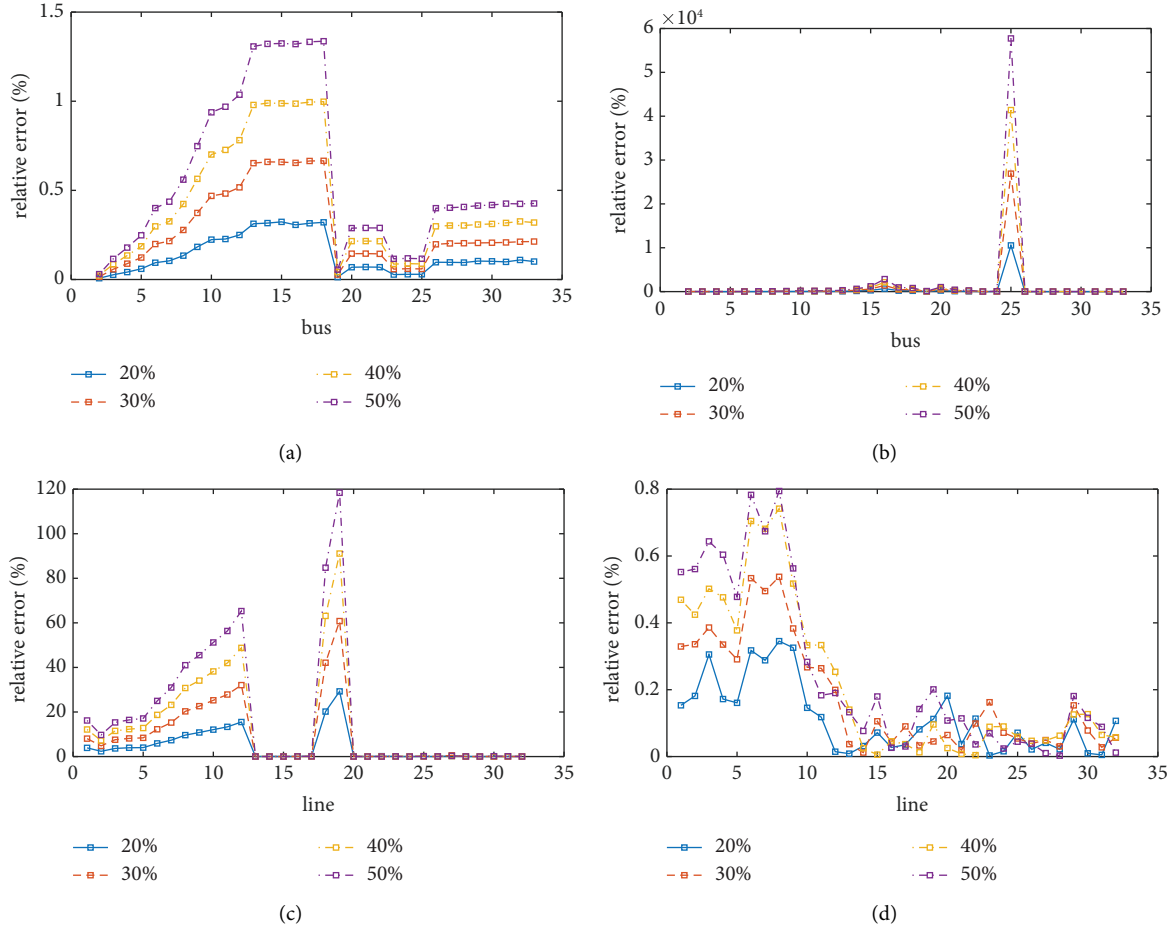
Figure 9: The value of $X_*$ with different penetrations of WT. (a) $V_m$. (b) $V_a$. (c) $P_{line}$. (d) $Q_{line}$.

In order to facilitate the observation, we reduced the mean value of $X_*$ of $V_a$ by 1/200. It is obvious that, when the variation range of fuzzy parameters is enlarged, the mean value of $X_*$ of the state variables increases correspondingly.

To see this phenomenon from probability view, the authors plot the PDF and CDF images of bus 10 in Figure 7. It is clear to see that the boundaries of cluster of the PDF and CDF curves expand to the left and right as the fuzzy parameter ambiguity increases. This is the result of the fuzziness of the input variables being passed through the system to the output variables.

*4.2. Analysis of Sensitivity.* In order to analyze which renewable energy has the greatest impact, just one kind of fuzzy parameters is relatively larger, for example, we only enlarge the range of fuzzy factor of WT to $(85\%, 117\%)$, while that of PV and load maintain $(99\%, 101\%)$.

Then, taking the result of the condition as a reference where all the three kinds of fuzzy factors are set to $(99\%, 101\%)$, and calculating the absolute errors of state variables between the enlarged condition and the reference condition. For the convenience of comparison, the absolute errors are processed as (23), and the results are shown in Figure 8.

$$X_{abs} = \left| \frac{X_{large,i} - X_{ref}}{P_{rate,i}} \right|, \quad (23)$$

where $X_{abs}$ denotes the absolute errors after processing, $X_{large,i}$ and $X_{ref}$ are $E_{pro-fuz}(Z)$ of state variables $Z$ of enlarged condition and reference condition and $i \in \{WT, PV, Load\}$. $P_{rate,i}$ is the rated output of WT or PV or the active power of load.

As shown in Figure 8, we can find that, changes in the fuzzy parameters of load, WT, or PV all have an impact on state variables. And in the figures of $V_a$ and $P_{line}$, the impact of WT and PV is more obvious than that of load at most of the places. This is due to the fact that WT and PV directly inject active power into the system, and active power is strongly correlated with $V_a$. In the figures of $V_m$ and $Q_{line}$, this phenomenon also occurs in the places close to WT and PV. That is, the closer a location is to WT and PV, the more vulnerable it is to their fluctuation. Therefore, with more and more renewable energy access systems, it is more meaningful to study the fuzziness of WT and PV than load.

*4.3. Influence Analysis of Penetration of WT.* In this section, the penetration of WT changes from 20% to 50%, while the other parameters remain unchanged and the value of $X_*$ of
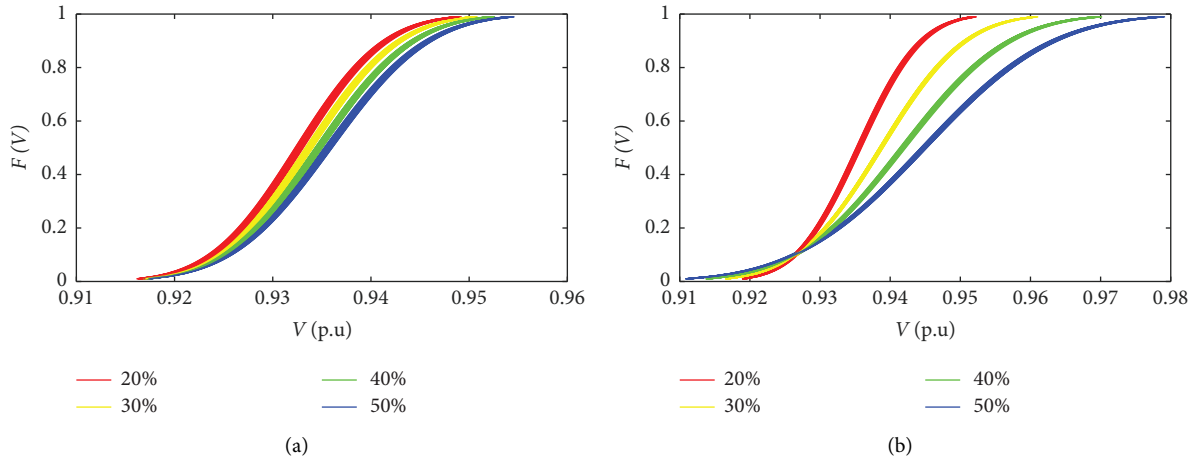
FIGURE 10: The CDF curves of $V_m$ with different penetrations of WT. (a) Bus 33. (b) Bus 13.

state variables is shown in Figure 9. It is obvious that the values of $X_*$ of all variables increase in general with the development of penetration, but increase mostly near renewable energy access points.

Thus, we select bus 33 and bus 13 which are far from and near points, respectively, to plot the CDF curves of $V_m$ as shown in Figure 10.

From the point of view of randomness, the CDF curve clusters all have a certain degree of displacement, and the displacement of the near point (bus 13) is more than that of the far point (bus 33). Therefore, the state variables of the near point have the risk of exceeding the limit and need to be paid more attention.

From the fuzzy point of view, the increase in the penetration of WT does not lead to a significant increase in the bandwidth of the CDF curve clusters. Combined with the abovementioned analysis, it can be seen that the change of the fuzzy number range of output variables lies more in the range of fuzzy number of input variables, and has less relationship with the penetration of renewable energy.

## 5. Conclusion

To analyze the influence from the two type of uncertainties produced by renewable energy and load demands penetrated in power systems, this study has established the random fuzzy model of WT, PV, and load, and combined the three point estimate method and random fuzzy simulation technology to calculate the random fuzzy power flow. The proposed method has been tested on the IEEE-33 system, and the following conclusions have been verified by the simulation results:

(1) The proposed 3PE-RFS has relatively faster calculation speed than MCS-RFS, and maintains high accuracy

(2) Compared with the traditional probability analysis method, more information of the power flow can be provided by the RFPF, in terms of mean, variance, PDF and CDF of the output variables,

(3) With the expansion of the fuzzy parameter range of input variables, the mean value of $X_*$ increases correspondingly, and at the same time, the boundaries of clusters of CDF expand to the left and right

(4) The fluctuation of renewable energy and load demands causes noticeable changes of state variables, and with more and more renewable energy access systems, it is more meaningful to study the fuzziness of WT and PV than load

(5) With the development of penetration of WT, the near points have the risk of exceeding the limit and need to be paid more attention. But there is no significant increase in the bandwidth of the CDF curve clusters. Therefore, the change of the fuzzy number range of the output variables lies more in the fuzzy number range of the input variables, and has less relationship with the penetration of renewable energy.

## Data Availability

The figures and tables used to support the findings of this study are included in the article. The data used to simulation are available at (https://doi.org/10.1049/iet-rpg.2017.0696). These prior studies are cited at relevant places within the text as mentioned in reference [35].

## Conflicts of Interest

The authors declare that there are no conflicts of interest regarding the publication of this paper.

## Acknowledgments

# References

[1] Z. Zhang and C. Kang, "Challenges and prospects for constructing the new-type power system towards a carbon neutrality future," *Proceedings of the CSEE*, vol. 42, pp. 2806–2819, 2022.

[2] R. Atassi and K. Yang, "An integrated neutrosophic ahp and topsis methods for assessment renewable energy barriers for sustainable development," *International Journal of Neutrosophic Science*, vol. 18, pp. 157–173, 2022.

[3] Y. Zhang, *Power system upgradingstate grid chief engineer chen guoping: a major historical opportunity for comprehensive transformation and upgrading of the power system*, pp. 28–31, state grid, Beijing, China, 2021.

[4] L. Ning, T. Yuan, and H. Wu, "New power system based on renewable energy in the context of dual carbon," *International Transactions on Electrical Energy Systems*, vol. 2022, Article ID 6428791, 8 pages, 2022.

[5] J. Zheng, J. Guo, Z. Li, Q. H. Wu, and X. Zhou, "Optimal design for a multi-level energy exploitation unit based on hydrogen storage combining methane reactor and carbon capture, utilization and storage," *Journal of Energy Storage*, vol. 62, Article ID 106929, 2023.

[6] C. Guo, Z. Liu, and B. Feng, "Research status and prospect of new-type power system risk assessment," *High Voltage Engineering*, vol. 48, pp. 3394–3404, 2022.

[7] C. Kang and L. Yao, "Key scientific issues and theoretical research framework for power systems with high proportion of renewable energy," *Automation of Electric Power Systems*, vol. 41, no. 9, pp. 2–11, 2017.

[8] Y. Liu, Z. Li, W. Wei, J. H. Zheng, and H. Zhang, "Data-driven dispatchable regions with potentially active boundaries for renewable power generation: concept and construction," *IEEE Transactions on Sustainable Energy*, vol. 13, no. 2, pp. 882–891, 2022.

[9] X. Fu and Y. Zhou, "Collaborative optimization of PV greenhouses and clean energy systems in rural areas," *IEEE Transactions on Sustainable Energy*, vol. 14, no. 1, pp. 642–656, 2023.

[10] N. Luo, J. Langevin, and H. Chandra-Putra, S. H. Lee, Quantifying the effect of multiple load flexibility strategies on commercial building electricity demand and services via surrogate modeling," *Applied Energy*, vol. 309, Article ID 118372, 2022.

[11] L. Wang, J. Zheng, Z. Li, Z. Jing, and Q. Wu, "Order reduction method for highorder dynamic analysis of heterogeneous integrated energy systems," *Applied Energy*, vol. 308, Article ID 118265, 2022.

[12] J. Zheng, W. Xiao, C. Wu, Z. Li, L. Wang, and Q. Wu, "A gradient descent direction based-cumulants method for probabilistic energy flow analysis of individual-based integrated energy systems," *Energy*, vol. 265, Article ID 126290, 2023.

[13] X. Fu, Q. Guo, and H. Sun, "Statistical machine learning model for stochastic optimal planning of distribution networks considering a dynamic correlation and dimension reduction," *IEEE Transactions on Smart Grid*, vol. 11, no. 4, pp. 2904–2917, 2020.

[14] W. Wu, Y. Feng, B. Zhang, and H. Wang, "Power system operation risk assessment based on credibility theory," in *Proceedings of the 4th China Annual Conference on Uncertain Systems*, pp. 66–81, Guilin, China, 2006.

[15] B. Liu and P. Jin, "Credibility theory - the axiomatic basis of fuzzy sets," in *Proceedings of the Second Annual Conference on Uncertain Systems*, pp. 7–17, Qinhuangdao, China, 2004.

[16] B. Borkowska, "Probabilistic load flow," *IEEE Transactions on Power Apparatus and Systems*, vol. PAS-93, no. 3, pp. 752–759, 1974.

[17] A. Da Silva, V. L. Arienti, and R. N. Allan, "Probabilistic load flow considering dependence between input nodal powers," *IEEE Transactions on Power Apparatus and Systems*, vol. PAS-103, no. 6, pp. 1524–1530, 1984.

[18] N. D. Hatziargyriou, T. S. Karakatsanis, and M. P. Papadopoulos, "Probabilistic load flow in distribution systems containing dispersed wind power generation," *IEEE Transactions on Power Systems*, vol. 8, no. 1, pp. 159–165, 1993.

[19] K. Jin, "Probabilistic energy flow algorithms for integrated electricity and natural gas energy system considering uncertainties of wind power output and load," M.Sc. thesis, Beijing Jiaotong University, Beijing, China, 2019.

[20] F. Ruiz-Rodriguez, J. Hernández, and F. Jurado, "Probabilistic load flow for photovoltaic distributed generation using the Cornish-Fisher expansion," *Electric Power Systems Research*, vol. 89, pp. 129–138, 2012.

[21] H. Khorsand and A. R. Seifi, "Probabilistic energy flow for multi-carrier energy systems," *Renewable and Sustainable Energy Reviews*, vol. 94, pp. 989–997, 2018.

[22] V. Miranda, A. Manuel, and C. C. Matos, "Distribution system planning with fuzzy models and techniques," in *Proceedings of the 10th International Conference on Electricity Distribution*, vol. 6, pp. 472–476, Brighton, UK, May 1989.

[23] V. Miranda and J. Saraiva, "Fuzzy modelling of power system optimal load flow," *IEEE Transactions on Power Systems*, vol. 7, no. 2, pp. 843–849, 1992.

[24] P. Chen, *Research on Interval Analysis Method for Uncertain Power Flow in Distribution Network with Renewable Energy*, M.Sc. thesis, North China Electric Power University, Beijing, China, 2019.

[25] P. R. Bijwe and G. Viswanadha Raju, "Fuzzy distribution power flow for weakly meshed systems," *IEEE Transactions on Power Systems*, vol. 21, no. 4, pp. 1645–1652, 2006.

[26] Q. Sun, H. Zhang, and Z. Liu, "Fuzzy flow calculation in power distribution system and its convergence," *Proceedings of the CSEE*, vol. 28, no. 10, pp. 46–50, 2008.

[27] D. Anuradha, T. K. Buvaneshwari, and M. M. Bhatti, "Solving stochastic fuzzy transportation problem with mixed constraints using the weibull distribution," *Journal of Mathematics*, vol. 2022, Article ID 6892342, 11 pages, 2022.

[28] J. Zhao, J. Li, and K. Abdullah, "Alzahrant and Jian Jia. "Research on stochastic fuzzy differential equations in multiple blurred image repair models"," *Fractals*, vol. 30, no. 02, Article ID 2240076, 2022.

[29] M. A. El Sayed, I. A. Baky, and P. Singh, "A modified topsis approach for solving stochastic fuzzy multi-level multi-objective fractional decision making problem," *Opsearch*, vol. 57, no. 4, pp. 1374–1403, 2020.

[30] B. Liu, *Studies in Fuzziness and Soft Computing*, Spring Berlin, Berlin, Germany, Heidelberg, 2 edition, 2009.

[31] R. Ma, Q. Zhang, X. Wu, and X. Li, "Random fuzzy uncertain model for daily wind speed," *Proceedings of the CSEE*, vol. 35, no. 24, pp. 6351–6358, 2015.

[32] R. Ma, W. Li, X. Li, X. Wu, and Z. Qin, "Random fuzzy model for load of distributed combined cooling, heating and power system," *Automation of Electric Power Systems*, vol. 40, no. 15, pp. 53–58, 2016.

[33] Z. Liu, Z. Wei, G. Sun, H. Zang, and Y. Li, "Probabilistic power flow calculation of power system with wind farms considering fuzzy parameters," *Power System Technology*, vol. 41, no. 7, pp. 2308–2318, 2017.

[34] G. Yang, P. Dong, M. Liu, and H. Wu, "Research on random fuzzy power flow calculation of ac/dc hybrid distribution network based on unified iterative method," *IET Renewable Power Generation*, vol. 15, no. 4, pp. 731–745, 2021.

[35] H. Wu, P. Dong, and M. Liu, "Random fuzzy power flow of distribution network with uncertain wind turbine, pv generation, and load based on random fuzzy theory," *IET Renewable Power Generation*, vol. 12, no. 10, pp. 1180–1188, 2018.

[36] G. Tsekouras and D. Koutsoyiannis, "Stochastic analysis and simulation of hydrometeorological processes associated with wind and solar energy," *Renewable Energy*, vol. 63, pp. 624–633, 2014.

[37] Z. Bie, P. Zhang, G. Li, B. Hua, M. Meehan, and X. Wang, "Reliability evaluation of active distribution systems including microgrids," *IEEE Transactions on Power Systems*, vol. 27, no. 4, pp. 2342–2350, 2012.

[38] L. Hong, L. Shi, L. Yao, B. Masoud, and Y. Ni, "Fuzzy modelling and solution of load flow incorporating uncertainties of wind farm generation," *Transactions of China Electrotechnical Society*, vol. 25, no. 08, pp. 116–112+130, 2010.

[39] S. Xu, "Distribution system reliability assessment considering multiple uncertainties correlations," M.Sc. thesis, Shanghai Jiao tong University, Shanghai, China, 2020.

[40] J. M. Morales and J. Pérez-Ruiz, "Point estimate schemes to solve the probabilistic power flow," *IEEE Transactions on Power Systems*, vol. 22, no. 4, pp. 1594–1601, 2007.

[41] B. Liu, R. Zhao, and G. Wang, *Uncertain Programming with Applications*, Tsinghua University Press, Beijing, China, 2003.

[42] Y. Feng, W. Wu, B. Zhang, H. Sun, and Y. He, "Power system operation risk assessment based on credibility theory part three engineering application," *Automation of Electric Power Systems*, vol. 30, no. 3, pp. 11–16, 2006.